

Accepted Manuscript

Journal of the Geological Society

Basement reservoir plumbing: fracture aperture, length and topology analysis of the Lewisian Complex, NW Scotland

K.J.W. McCaffrey, R.E. Holdsworth, J. Pless, B.S.G. Franklin & K. Hardman

DOI: <https://doi.org/10.1144/jgs2019-143>

This article is part of the The Geology of Fractured Reservoirs collection available at:
<https://www.lyellcollection.org/cc/the-geology-of-fractured-reservoirs>

Received 23 August 2019

Revised 21 May 2020

Accepted 10 June 2020

© 2020 The Author(s). This is an Open Access article distributed under the terms of the Creative Commons Attribution 4.0 License (<http://creativecommons.org/licenses/by/4.0/>). Published by The Geological Society of London. Publishing disclaimer: www.geolsoc.org.uk/pub_ethics

Supplementary material at <https://doi.org/10.6084/m9.figshare.c.5017139>

When citing this article please include the DOI provided above.

Manuscript version: Accepted Manuscript

This is a PDF of an unedited manuscript that has been accepted for publication. The manuscript will undergo copyediting, typesetting and correction before it is published in its final form. Please note that during the production process errors may be discovered which could affect the content, and all legal disclaimers that apply to the journal pertain.

Although reasonable efforts have been made to obtain all necessary permissions from third parties to include their copyrighted content within this article, their full citation and copyright line may not be present in this Accepted Manuscript version. Before using any content from this article, please refer to the Version of Record once published for full citation and copyright details, as permissions may be required.

Basement reservoir plumbing: fracture aperture, length and topology analysis of the Lewisian Complex, NW Scotland

K.J.W. McCaffrey^{1,2}, R.E. Holdsworth^{1,2}, J. Pless¹, B.S.G. Franklin¹, K. Hardman^{1,3}

¹Department of Earth Sciences, Durham University, Durham, UK, DH1 3LE.

²Geospatial Research Ltd, Office Suite 7, Harrison House, 1 Hawthorn Terrace, Durham, DH1 4EL

³Energy and Environment Institute, Hull University, Hull, UK, HU6 7RX

Abstract

Upfaulted ridges of Neoproterozoic crystalline basement rocks formed in the Faeroe-Shetland basin as a consequence of Mesozoic rift processes and are an active target for oil exploration. We carried out a comprehensive fault and fracture attribute study on the extensive exposures of geologically equivalent crystalline basement rocks onshore in NW Scotland (Lewisian Gneiss Complex) as an analogue for the offshore oil and gas reservoirs of the uplifted Rona Ridge basement high. Our analysis shows a power-law distribution for fracture sizes (aperture and length), with random to clustered spacing, and high connectivity indices. Regional variations between the Scottish mainland and the Outer Hebrides are recognised that compare directly with variations observed along the Rona Ridge in the Faeroe-Shetland basin. Here we develop a model for the scaling properties of the fracture systems in which variations in the aperture attributes are a function of the depth of erosion beneath the top basement unconformity. More generally, the combination of size, spatial, and connectivity attributes we found in these basement highs demonstrates that they can form highly effective, well plumbed reservoir systems in their own right.

The metamorphic basement rocks of the Lewisian Gneiss Complex may once have seemed an unlikely target for hydrocarbons, but a series of recent discoveries means that they are now a focus for exploration activity in the Faeroe-Shetland basin (Fig. 1). The delineation of the Clair and Lancaster fields, and associated prospects confirms that there are significant oil accumulations in Neoproterozoic basement lithologies of similar age to the onshore Lewisian Gneiss Complex in NW Scotland. These crystalline basement ridges were uplifted and exposed at surface during Mesozoic rifting before being buried again during the Cenozoic Atlantic margin opening (Stoker *et al.* 2018). Given that permeability in basement reservoirs is predominantly fracture-controlled (e.g. Achtziger-Zupančič *et al.* 2017) and given the general uncertainty associated with fractured reservoir systems (Nelson 1985), a renewed interest in studying analogue basement-hosted fracture systems is unsurprising.

Well -exposed outcrops of the Lewisian Gneiss Complex occur in the mainland of NW Scotland and in the Outer Hebrides, the latter being an elongate uplifted crustal block with similar dimensions to the Rona Ridge offshore, and along-strike, where significant hydrocarbon discoveries have been made (Fig. 1).

Although rare, producing basement reservoirs in a range of fractured igneous and metamorphic host rocks are known from 27 countries worldwide (Gutmanis *et al.* 2009; 2015). They form by conventional means with migration from a mature basinal source rock into a fractured reservoir trap and are contained by a low permeability top seal. Oil accumulation in the crystalline basement of the Clair field has long been known (e.g., Coney 1993), but recent discoveries in other parts of the Rona Ridge, where basement has been specifically targeted include the Lancaster field, and the Lincoln, Halifax and Whirlwind prospects (Slightam 2012; Trice 2014).

The Lewisian Gneiss Complex of NW Scotland has, over its c. 3.2 Ga history, formed part of an active accretionary margin, a collisional foreland, a rifted margin (at least twice) and most recently a passive margin, and therefore retains a record of several generations of both ductile and

brittle deformation, metamorphism and fluid flow events. This complex history has produced a highly heterogeneous array of lithologies, metamorphic grades and structural styles (e.g. Park 1970).

Here, we present an analysis of fracture attribute datasets collected from brittle structures exposed across the onshore Lewisian Complex. The comprehensive nature of the data compilation (some 80 individual datasets) enables us to identify correlations between the mainland Lewisian and the Clair basement, and the Hebrides exposures with the Lancaster field. We then propose a simple model that accounts for the first order differences in fracture attributes and their scaling that is linked to recent work on the geological nature and development of the fracture systems and their infills (Holdsworth *et al.* 2019a, b, Trice *et al.* 2019). This work has led to a new understanding of the significance of fissuring processes in enhancing the capability of uplifted rift blocks of fractured crystalline basement to host significant accumulations of hydrocarbons and also provides a general model for explaining fluid flow in other uplifted basement lithologies in similar settings below regional unconformities.

Geological Setting

Location and regional structure

The Precambrian rocks of the Lewisian Gneiss Complex of NW Scotland form a fragment of the continental basement of Laurentia that was isolated from North America by the opening of the North Atlantic (Bridgwater *et al.* 1973). The rocks comprise trondjemitic, tonalitic and granodioritic orthogneisses, with subordinate units of metabasic-ultrabasic and granitic composition, together with local units of metasedimentary rock. The complex then underwent a long history of major, crustal-scale geological events during the Archaean and Palaeoproterozoic (see Wheeler 2010 and references therein) and is divided into a number of tectonic regions or 'terranes' that are separated by mainly steeply-dipping shear zones or faults.

Two different tectonic views exist concerning the early geological evolution of the Lewisian Gneiss Complex. The first, based on the classic geological mapping by Sutton and Watson (1951), suggests that much of the basement gneiss is a single piece of continental crust that shares a common early history. This model was rooted in the recognition of two fundamentally separate groups of tectonothermal events, one predating and one postdating the intrusion of a regional swarm of NW-SE trending mafic to ultramafic dykes known as the Scourie Dyke swarm (Sutton and Watson 1951). Areas where evidence for these early events is not preserved were thought to have undergone intense overprinting and reworking during later Paleoproterozoic events ('Laxfordian'). A more recent alternative hypothesis, proposed by Friend and Kinny (2001) and Kinny *et al.* (2005), is founded in zircon geochronology and suggests that each terrane has different Archaean age spectra. They view the Lewisian as a collage of lithologically and geochronologically distinct tectonic units or terranes bounded by regional shear zones that were assembled progressively during a series of Precambrian amalgamation episodes.

Neoarchaean orthogneisses of broadly similar composition and age extend north of the Scottish mainland at least as far as the northernmost tip of Shetland (Holdsworth *et al.* 2018; Kinny *et al.* 2019). Equivalent units underlie much of the Faroe-Shetland basin and the ca 200km Rona Ridge, as shown by analyses of basement-penetrating offshore cores (Fig 1; see Ritchie *et al.* 2011). These basement rocks have protoliths and early amphibolite facies tectonothermal events of broadly the same age as those of the Lewisian Gneisses (ca. 2.8-2.7Ga), but lack the Palaeoproterozoic (Laxfordian) overprinting events (Holdsworth *et al.* 2018). These rocks are directly comparable to those of the North Atlantic Craton in Eastern Greenland and Canada, whilst the reworked rocks of the Lewisian Gneiss Complex in NW Scotland and the Hebrides are thought to be southeasterly equivalents of the Nagssugtoqidian gneisses of Eastern Greenland (Mason & Brewer, 2004; Holdsworth *et al.* 2018).

Early metamorphic assemblages and structures, together with the Scourie dykes, are heterogeneously overprinted by Laxfordian reworking in parts of the Lewisian Gneiss Complex. These older features are only clearly preserved in certain areas of the mainland complex, most notably the 'Central Region' or Assynt Terrane (Fig 2). The main phases of the Laxfordian deformation and metamorphism predominate in the Rhiconnich and Gruinard terranes that lie to the north and south of the Assynt Terrane respectively (Fig. 2). The NW-SE strike-slip-dominated shear zones that form the terrane boundaries on the Scottish mainland – and another 1 km wide structure in the centre of the Assynt Terrane known as the Canisp Shear Zone (Fig 2) - are thought to have formed and perhaps initially juxtaposed the three terranes during an early (Inverian) event ca 2.4 Ga (Park *et al.* 2002). All were then reactivated during episodic Laxfordian shearing (ca 1.9-1.66 Ga) often with alternating shear senses (Park *et al.* 2002). The predominantly amphibolite facies granodioritic orthogneisses of the Outer Hebrides, preserve a superficially similar relative chronology of structures and metamorphic assemblages as on the mainland.

Faulting and fracturing history

Currently exposed levels of the Lewisian Gneiss Complex passed through the brittle-ductile transition at some point after ca. 1.66 Ga and were close to the surface by ca. 1.2 Ga, the depositional age of the unconformably overlying, unmetamorphosed Stoer Group on the Scottish mainland (Beacom *et al.* 2001; Holdsworth *et al.* 2020). Unsurprisingly for rocks that preserve a record of brittle deformation processes that occurred across a range of crustal depths, the Lewisian displays a wide range of micro- to regional-scale brittle fractures. A broad spectrum of types is developed that are difficult to strictly separate using an arbitrary classification scheme (Pless 2012, Franklin 2013). These include the following:

Joints are predominantly Mode 1-type tensile fractures based on a general lack of observed offsets of pre-existing features such as compositional banding. They are typically closed and only become open due to the effects of weathering - either in the geological past or present day - or due to later

tectonic processes (such as fissuring – see below). They occur on a variety of scales but, like many Mode 1 fractures developed in crystalline basement rocks worldwide (e.g. Wang *et al.* 2019), are commonly of large lateral extent both horizontally and vertically (Fig. 3a).

Veins are dominantly mm- to m-scale tensile or hybrid fractures filled with a variety of hydrothermal minerals including (commonly) quartz, epidote, carbonates (calcite, siderite), chlorite, K-feldspar (adularia), iron oxides and (less commonly) base metal sulphides, prehnite and a variety of zeolites (Fig. 3b). The majority are entirely occluded by their mineral fills, but in some cases, partial fills and vuggy textures are preserved. Like many basement terrains, veins completely filled with dark, aphanitic pseudotachylyte (friction melts) are well developed locally and are typically associated with fault zones formed relatively early in the brittle deformation history (e.g. Imber *et al.* 2001; Holdsworth *et al.* 2020).

Fissures are mm to dm-scale dilational (predominantly Mode 1) fractures filled or partially filled with often complex, composite fills formed at a range of crustal depths. Many formed close to the surface in the geological past and are spatially associated with regional unconformities at the base of the Torridonian or Mesozoic cover sequences (e.g. Beacom *et al.* 1999; Jonk *et al.* 2004). Fills here include wall rock collapse breccia, hydrothermal minerals, and fine-grained sediment, sometimes with a laminated structure and cement consistent with having been deposited by flowing water in subterranean open cavity systems (Fig 3c, d). Deeper fissure fills include magma, i.e. Palaeozoic to Cenozoic dykes, and wall rock collapse breccias mixed with friction melt and hydrothermal minerals (Fig 3c, e).

Shear fractures range from simple ‘clean break’ brittle faults with sub-mm-scale offsets through to large complex *fault zones* with km-scale offsets. Fault rocks typically begin to appear once displacement exceeds more than a few mm, and include early-formed pseudotachylytes and cataclasites, breccias, and gouges; all with associated hydrothermal mineral assemblages similar to

those seen in associated vein systems. Fault rocks formed earlier in the brittle deformation history are generally cohesive and highly indurated whilst those formed later and nearer to the surface are typically incohesive and easily weathered. Polished fault surfaces with slickenlines or hydrothermal mineral slickenfibres – particularly of quartz, epidote, chlorite or carbonate – are widely preserved (Fig 3f). Large-scale fault zones – such as the Seaforth Fault in Lewis (Fig. 2; Franklin 2013) are typified by the development of well-defined cores with foliated gouges (Fig 3g) and broad, chaotically fractured damage zones (e.g. Pless *et al.* 2015). Some – but not all - show evidence of reactivation (e.g. Imber *et al.* 2001; Holdsworth *et al.* 2020).

A long history of fracturing is recognized on the Scottish mainland with *at least* three main fault/fracture sets preserved in the foreland region west of the Caledonian Moine Thrust zone (Fig. 2). Each is associated with different fault geometries, kinematics and fault rock assemblages. These are (from earliest to latest):

- 1) NW-SE 'Assyntian' or 'Late Laxfordian' sinistral fault arrays (Holdsworth *et al.* 2020) which are most abundant as reactivation events in pre-existing NW-SE Laxfordian shear zones (e.g. Canisp shear zone, Fig 2) and along the margins of pre-existing Scourie Dykes (Beacom *et al.* 2001; Pless 2012). These structures are associated with the development of cohesive cataclasites and pseudotachylytes. Their Mesoproterozoic (ca. 1.55 Ga) age is constrained by Re-Os dating of associated copper sulphide mineralization in the Assynt terrane (Holdsworth *et al.* 2020) and they demonstrably predate deposition of the unconformably overlying Stoer Group ca 1.2 Ga. A generally N to NE-trending set of complex polymodal fracture arrays was thought by Beacom *et al.* (1999, 2001) to be associated with the Stoer Group age rifting, but more recent fieldwork and thin section analysis (Hardman 2019) have shown that these fractures are synchronous with the NW-SE structures. The NE-SW structures are commonly associated with dilation and collapse brecciation, pseudotachylyte injection and epidote mineralisation that pre-dates Stoer Group deposition (Holdsworth *et al.* 2020).

- 2) Post-Torridonian (ca 1.04 Ga) faults, including isolated thrusts and strike slip faults related to the Palaeozoic Moine Thrust Zone; many of the NW-SE Late Laxfordian faults also show evidence of reactivation close to the thrust belt (Krabbendam & Leslie 2010; Pless 2012). Most are clean breaks or are associated with the development of well-cemented breccia and gouge. Multiple sets of microfractures and fills of mainly Palaeozoic age may also be present (e.g. Laubach & Diaz-Tushmann 2009; Ellis *et al.* 2012).
- 3) Mesozoic age structures that are generally NE-SW and NW-SE-trending dip-slip & strike-slip fracture sets that are widely associated with incohesive gouges & carbonate mineralization (Laubach & Marshak 1987). Many of the fissure structures are thought to have formed during Mesozoic rifting events when the basement was at or close to surface. These structures are likely more widespread than has generally been assumed and they typically show little evidence for reactivation except along major faults (e.g. Coigach Fault; Roberts & Holdsworth 1999). Holford *et al.* (2010) showed that NW Scotland has experienced multiple episodes of Mesozoic and Cenozoic burial and exhumation associated with passive margin formation, rifting processes and inversion.

The early brittle faulting history of the Outer Hebrides is dominated by the development of the SE-dipping Outer Hebrides Fault Zone (OHFZ) that initially developed as a mylonitic shear zone possibly of Laxfordian or Grenvillian age (Imber *et al.* 2001, 2002) (Fig. 2). It then experienced a series of reactivation events from the Neoproterozoic to the Mesozoic, but direct geological or radioisotopic evidence for the age of movements is sparse. The likely presence of Torridonian rocks within Minch Basin (Figure 2) suggests that the OHFZ may have been active as a normal fault ca. 1.04 Ga, but there is no clear record of this faulting yet recognized in outcrops. Onshore, post-mylonite deformation along the OHFZ was initially brittle and was associated with the development of pseudotachylite-bearing fault veins and thick, SE- to E-dipping pseudotachylite-ultracataclasite crush zones all along the eastern margin of the Hebridean island chain (e.g. Sibson 1977). The brittle

faults & crush zones are overprinted by a network of macroscopically ductile, greenschist facies phyllonitic shear zones that developed due to the influx of hydrothermal fluids during top-to-the-NE sinistral strike-slip shearing along the OHFZ (Butler *et al.* 1995; Imber *et al.* 2001). These shear zones were themselves then reactivated during late Caledonian brittle-ductile top-to-the-E extensional deformation (Imber *et al.* 2001). The Permo-Triassic Stornoway Formation (Steel *et al.* 1975) was deposited in eastwardly-prograding alluvial fans associated with normal fault scarps developed in hangingwall of the OHFZ (Fig 2). The sedimentary sequence contains clasts of basement gneisses and OHFZ-derived fault rocks, suggesting that the northern Outer Hebrides was exhumed by the earliest Mesozoic era. The rocks of both the Lewisian Gneiss Complex (including the OHFZ) and the Stornoway Formation are cut by E-W, NW-SE and NE-SW fractures, some of which – together with generally NNW-trending Tertiary dykes, form prominent topographic lineaments (e.g. Loch Seaforth) (Fig. 2) (Franklin 2013). Faulting events are widely associated with the development of generally incohesive gouge, breccia and fissure fills with local widths of at least 30m, but perhaps up to 100m, together with extensive carbonate mineralization. The Tertiary dykes mostly cross-cut the faults and fault rocks which are assumed therefore to be of Mesozoic age, but some fault sets show evidence of significant post-dyke reactivation during the Cenozoic, notably a prominent set of E-W trending structures which are also characterized by a later phase of milky carbonate mineralization (Franklin 2013).

Methodologies

Sampling of fault and fracture networks

The datasets reported in this study were mainly acquired using the 1D linear scanline method (Priest & Hudson 1981; Baecher, 1983; McCaffrey & Johnston, 1996; Ortega *et al.* 2006). This method allows a relatively simple characterization, albeit with known biases, of fracture sizes and intensities,

and generally can be deployed at most field localities. The data (observations along a sample line) are closely analogous to logs from borehole or drill core taken from a prospect or reservoir. To gain 2D (map) information on the spatial and topological relationships within the fractured system, we also conducted 2D window sampling (Odling 1992; Mauldon *et al.* 2001; Rohrbaugh *et al.* 2002; Zeeb *et al.* 2013; Watkins *et al.* 2015; Sanderson and Nixon, 2015), enabling access to connectivity estimates for the fracture array, which are a key input for modelling fluid-flow.

For the linear scanlines, fracture orientations, lengths and apertures, together with composition and texture of fracture infills and fracture terminations on joints and other faults were recorded at measured intervals along the sample line. The start and end point of each transect was recorded using a hand-held GPS unit. Most of the fractures are filled, or partially filled with minerals (mainly quartz, epidote or calcite) and, following Laubach (2003) and Ortega *et al.* (2006), the apertures measured in this study are the opening displacement where the scan line intersects the fracture including any fill, i.e. the 'kinematic aperture'. This is equivalent to the fracture thickness of McCaffrey & Johnston (1996) and Massiot *et al.* (2015).

Fracture samples

The 1D datasets were collected in the field mainly from natural exposures of the Lewisian Gneiss Complex (well exposed in coastal settings), but also from road cuttings where natural fractures may be easily distinguished from those created by blasting (for detailed descriptions of the sample locations see Pless 2012 and Franklin 2013). The locations of study sites across the mainland Scotland and Hebrides are shown in Figure 2 with full details of individual sample lines given in the supplementary tables. The initial studies focused on size (aperture, length), spatial characterization (orientation and spacing) and the topological characteristics of the fracture systems. Our database contains more than 100 individual datasets (48 aperture and 29 length samples and 27 topological estimates) chosen because they capture the fracture systems that formed from Proterozoic to Cenozoic times (see above). Details of the fracture samples, including location, host lithology,

number of fractures, sample line length for 1D samples, area for 2D samples, types of structure intersected are given in the Supplementary file (Tables S1 and S2). To extend the analysis to other scales, the above-mentioned scanline methods were adapted and applied to aerial photographs and optical data (BGS NextMap data) to quantify fracture lengths in 1D (see lineaments shown on Figure 2). These datasets were collected before we had fully appreciated the importance and extent of fissure formation in the basement, particularly in the Hebrides, nonetheless we think the study provides important baseline information.

Data from the Clair field comprise fractures logged in wells 206/7a-2 and 206/8-8 that were drilled by Elf into crystalline basement gneisses of the Clair ridge (see Holdsworth *et al.* 2018 Fig. 2). Core samples were examined at the Iron Mountain core storage facility, Aberdeen and a fracture analysis was conducted by Pless (2012) and in this study. The basement core slab samples from 206/7a-2 are in 10m lengths at irregular intervals from measured depths of 2140m to 2600m (see Holdsworth *et al.* 2018 and S1).

At regional scales, a fracture interpretation of Clair 3D top basement seismic attribute maps was performed (see Pless 2012 and Fig. 2 inset). From this fracture map we were able to derive fracture length distributions along 1D sample lines across the maps and in 2D windows. An equivalent study of fracture lengths in 1D and 2D was carried out on the onshore lineament maps from the mainland and Hebrides (see Fig. 2). The lineament maps show density variations related to the amount of younger cover rocks or Quaternary material (Fig 2) and so our length analyses were conducted on lines that cross, or windows that sample, regions with high density and thin cover. We carefully filtered the datasets to make sure that those with low numbers (c. $n < 40$) were omitted. We also checked that the datasets were collected and formatted in a comparable way as they have been assembled from a number of studies.

For the topology study, photographs from outcrops in the Assynt terrane, Clair core 206/7a-2 supplemented by samples from the 205/21-1A from further along the Rona Ridge (Lancaster field)

collected at BGS core store form the basis for picking of nodes and branches. All node and branch picking was carried out manually to ensure the correct network topology was recorded.

Data analysis

In this study we assessed the distribution of fracture size (aperture and length) attributes, collected from the 1-dimensional sample lines as a primary characterisation of the brittle deformation within the basement Lewisian Gneiss Complex. We collected fracture data from drill core samples from the basement of the Clair field for comparative purposes. We only report the aperture data here as the fracture lengths are heavily censored by the dimensions of the drillcore. However, we report regional scale 2D length data from onshore Lewisian terranes from the lineament dataset derived from the optical data that is equivalent in scale to the offshore seismic attribute maps. This allows us to constrain further the upscaling of fracture attribute and compare the offshore basement fracture mapping to that performed on seismic attribute maps.

Fracture sizes

Fracture intensity plotted as cumulative distribution (population) plots enables an assessment of the distribution, spatial and scaling properties of the fracture population (i.e. the ratio of small to large fractures for a given sample line length). Fracture attribute distributions display three main types of statistical distribution (Gillespie *et al.* 1993; Bonnet *et al.* 2001, Zeeb *et al.* 2013): (a) Exponential, random or Poisson distributions are characteristic of a system with a randomised variable; (b) Log-normal distributions are generally produced by systems with a characteristic length scale, for example layer-bound jointing (Narr, 1991 and Olson, 2007); (c) Power-law distributions lack a characteristic length scale in the fracture growth process (Zeeb *et al.* 2013) (see Supplementary file S1). Although some fracture populations are better described by scale-limited laws, such as log-normal or exponential distributions, it is generally accepted that power-law distributions and fractal geometry provide a widely applied descriptive tool for fracture system characterization (e.g. Bonnet

et al. 2001). Ideally, the best-fit power-law distribution should be constrained over several orders of magnitude (Walsh and Watterson, 1993; McCaffrey and Johnston, 1996). However, in practice this is typically very difficult to achieve at a given scale due to sampling limitations. Fracture sampling issues (e.g. censoring and truncation) are commonly encountered and can result in an incomplete description of the full population. For instance, when large fractures are incompletely sampled in a power-law population, the resulting plot can resemble a log-normal distribution. Following Ortega *et al.* (2006), Dichiarante *et al.* (2020) have shown how a multi-scale approach can be used to better constrain the scaling laws for fracture size attributes. As pointed out by Clauset *et al.* (2009), use of the maximum likelihood estimator (MLE) is preferred over a least square regression analyses (R^2) for the fitting of power-law distributions. In this study we used MLE scripts developed by Rizzo *et al.* (2017) as used in the FracPaQ toolbox (Healy *et al.* 2017). In addition, we followed the Dichiarante *et al.* (2020) modification in which the MLE for power-law, exponential and log-normal fits are calculated on systematically truncated and censored datasets to find the optimum distribution parameters (see S1).

Fracture spatial organization

The spatial organisation of fracture systems are a property of the orientation and clustering of fractures in 1D sample lines. For many years the Coefficient of Variation (C_v) - the standard deviation of all spaces between adjacent fractures divided by the mean spacing (Gillespie *et al.* 1993; 1999) - has been used as to describe clustering. These authors showed that a $C_v > 1$ reflected a clustered distribution and could be expected in non-layered rocks (like basement). A random or Poisson distribution gives an exponential ($C_v = 1$). Superimposition of power law distributions can give a 'Kolmogorov' distribution (log-normal) ($C_v < 1$). Log-normal (and normal distributions) are also produced by 'saturation' models when fractures are produced in well bedded sequences (Bai *et al.* 2000). The C_v values for 1D basement sample lines are reported in this study, however we note that there are issues with the sensitivity of this method and that the method does not taken into account the size of structures or the scale of clustering (Marrett *et al.* 2018). The correlation analysis

method subsequently developed by Marrett *et al.* (2018) is now the preferred method for analysing fracture spatial distributions and will be the subject of further work on the datasets collected in this study.

Fracture topology

While the 1D scanline data provides information about fractures as single entities and their distribution, 2D topology analyses consider fractures as part of a network and provide access to fracture connectivity assessment. The 2D analysis used here has been carried out on fracture maps at regional scale (metre-decametre) DEM images and seismic attribute maps (see Fig 2). At smaller scales (centimeter-metre) we carried out topological analysis on core samples and outcrops. We followed the methodology of Sanderson and Nixon (2015) in defining nodes and branches. 'Nodes' are defined as the point where a fracture terminates (I-type), abuts against/splays from another fracture (Y-type) or intersects (cross-cuts) another fracture (X-type). 'Branches' are the portions of a fracture confined between two nodes.

The number of nodes and branches for a given fracture network is strictly related, meaning that by knowing one of the two elements for the fracture network, it is possible to quantify all its components. NI, NY and NX are defined as the number of I-, Y- and X-type nodes and PI, PY and PX their relative proportions. Once the number of nodes and/or branches making up a fracture array are known, the connectivity can be visualized using a ternary plot of the component proportions or can be quantified by calculating the number of connections existing in the 2D map. In general, X-type nodes provide 4 times and Y-type nodes 3 times more connectivity than I-type nodes (Sanderson and Nixon 2015). An array dominated by I-nodes is isolated, while arrays dominated by Y- and X-type nodes are increasingly more connected.

Results

Fracture lineaments from the Mainland (Assynt and Rhiconnich) terranes show strong NE-SW and WNW-ESE trends (Pless 2012; Fig. 2). In contrast in the Hebrides, the main lineament trend is NNW-SSE with a subordinate ENE-WSW trend (Franklin 2013; Fig. 2). The lineament maps show density variations that particularly reflect the amount of Quaternary cover, e.g. see southern and western Lewis compared to the northern region (Fig. 2). At the regional scale, there is no qualitative variation in density of lineaments in relation to major structures such as the Outer Hebrides fault zone, Canisp Shear zone or the Seaforth fault (Fig. 2). We also see no systematic variation at this scale with the host lithological units (Fig. 2). Pless et al (2012) has conducted an analysis of fracture density maps which confirms the qualitative observations.

Aperture data

Figure 4 shows cumulative distribution plots for the aperture distributions for localities in Lewisian Complex gneisses on the Mainland (20 sample lines), Hebrides (17 lines) and Clair basement core (12 lines). Details of the individual samples and the distribution fitting parameters are given in Table S1. For the Mainland, there is high degree of variability, but the data span more than 3 orders of magnitude from 0.00005m to 0.5m (0.05-500mm) in aperture (Fig. 4a). We note that some constant values appear in the plots at small sizes and are a rounding effect that occurs during the field acquisition. We generally remove repeated values, as recommended by Ortega *et al.* (2006), but the application of the Terzhagi true thickness correction tends to smear out these clusters of sub-mm values towards even smaller values. In terms of the fracture intensity or spacing (y axes), the data show about an order of magnitude spread from low strain (0.05 fractures of 10 mm size per metre) to high strain (1 x 10 mm fracture per metre) (Fig. 4a). For the Hebrides, data span nearly 5 orders of magnitude from about 0.05 mm to 1000mm (Fig. 4b). Fracture intensity or spacing (y axes) vary by about an order of magnitude from 0.1 x 10mm fracture per metre to higher strain of about 2 x 10 mm per metre. For the Clair core datasets, aperture values range from 0.05mm to 100mm and the

intensity values are less variable than the onshore datasets ranging from 0.5 to 1.2 per metre for 10mm aperture fractures.

Aperture distribution data for all regions can be described by power-law scaling or log normal distributions with greater than 95% confidence calculated using the MLE method with a slight preference for power-law distributions (Fig. 4 and Table S1). The sample lines (Garrabost, Memorial Cairn, Pabail and Seisadar) identified by Franklin (2013 and Supplementary file S1) are those taken across Mesozoic structures and tend to be those that display the highest absolute aperture values (Fig. 4).

The advantage of plotting many datasets together (Fig. 4) is that general trends emerge above variations displayed by individual samples (see Discussion below). One clear signal that emerges is that the power law exponent is lower for samples from the Hebrides than for the Mainland and the Clair basement. This can be seen qualitatively in Figure 4. For the Mainland and Clair data (Fig. 4a), the averages lie along the grey shaded reference area which has boundaries with a slope = -1 on the plot except at the lower and upper ranges where truncation and censoring effects are likely. For the Hebrides, the data sets clearly plot along a shallower slope line compared to the shaded reference area. To test this inference, we performed a significance test of the difference between the MLE power law scaling exponents (individual slope with > 95 % confidence fits) for the two regions. An average power law exponent for each region was calculated and the *t* test statistics confirm that the Mainland (average slope $\alpha = 1.23$, SD = 0.49) and Hebrides (average $\alpha = 0.74$, SD = 0.26) conditions; $t(37) = 4.15$, $p = 0.0002$ are different. These results show that the Hebrides and Mainland fractures show different scaling properties, and this implies that there are *fewer* small aperture fractures in the Hebrides relative to the largest fractures when compared to those seen in the Mainland.

Length distributions

The fracture length distributions for faults and fractures from both onshore and offshore regions are presented as cumulative distribution plots of intensity versus length in Figure 5. Length data at smaller scales from outcrops (c 0.1-10m) are plotted alongside line samples across the top Clair basement (c 0.5 -50 km) (Fig. 5a). Details of individual samples and distribution fitting are given in Table S2. Again, most of the samples can be described by power-law or log normal distributions with greater than 95% confidence with a slight preference for log normal distributions. A general scaling relationship (power-law) from outcrop to regional scale is suggested (Fig 5a).

The regional scale 2D length data from both onshore lineament mapping and offshore top basement seismic attribute map (Fig 2 inset) are shown in Figure 5b with details of distribution fitting given in Table S2. The data show good agreement between the onshore Lewisian and the Clair field (similar intensity values and slopes) at fracture lengths 1-50km (Fig. 5b). Below 0.5-1 km, the distributions show truncation effects (inflection points on the curves) that are dependent on the scale at which the fractures have been mapped and the level of exposure (onshore this is c. 500m and offshore it is c. 1 km).

Spatial organisation

The C_v values for the spaces between adjacent fractures for each sample lines are shown on Figure 6 plotted against the overall fracture intensity for each of the sample line datasets assembled in this study. Plotting in this way enables us to compare C_v values and assess the spatial organisation at different scales. The values show a range of behaviours from more uniform spacing (<1) to more clustered distributions (>1). There is a large amount of variation, but two overall observations may be suggested: 1) Regional-scale data tend to be more uniform and outcrop data more clustered (e.g. compare Clair regional and core C_v values); and 2) the Hebrides data show a tendency for more clustered spacing distributions compared to the Mainland (Assynt and Rhiconnich) terranes. Franklin (2013) indicated that this effect is most pronounced at the outcrop scale (Fig. 6) and is likely due to the prominent influence of Mesozoic faulting in the Hebrides region.

Topology results

The topology analyses were carried out on a range of onshore and offshore samples including drillcore, outcrop images, seismic attribute and regional datasets. Figure 7 shows a summary of the topology values that have been obtained from Clair and other Rona Ridge (Lancaster) core and the Assynt terrane (See Table S3 for full results). All basement samples show connected fracture networks with C_B values $\gg 1$ which is the threshold C_B (connections per branch) for a connected network. Most outcrop and core samples show a predominance of Y node-dominated fracture networks (Fig. 7).

Discussion

This study, which reports the largest attribute dataset ever assembled for basement-hosted fractures, shows that the Scottish mainland exposures broadly show similar scaling and connectivity properties to the Clair basement and the greater Rona Ridge. Aperture scaling from all three areas (Hebrides, Mainland and Clair) can be described by a power-law distribution when appropriate censoring and truncation of individual datasets are taken into account (Fig. 3 and Table S1). A number of individual datasets, which tend to be those with lower sample numbers, may be equally or slightly better described by log normal distributions. Fracture length datasets from both onshore and offshore may be described by either power-law or log normal distributions. Length distributions are known to be particularly prone to censoring and truncation (Odling *et al.* 1999). However, Odling *et al.* (1999) and Dichiarante *et al.* (2020) have shown that a multi-scale analysis can help to confirm that power-law scaling is an appropriate choice to model the fracture length distributions. In the present study, the basement fracture lengths sampled in 1D show a scaling relationship across 8 orders of magnitude and the 2D sample windows show consistent and comparable length distributions between onshore and offshore datasets. Fractures onshore and offshore show similar spatial characteristics as demonstrated by the C_v values. The fracture topology analyses show similar levels of connectivity between onshore and offshore basement terranes. We note that the fracture networks at three scales (regional, outcrop and core) from kilometre to centimetre scale appear to be strongly Y-node dominated, which supports the conclusions that the networks are all well

connected (Sanderson & Nixon 2015). Y-node dominated connectivity might be expected in relatively massive basement rocks which have multiple fracturing events in which large apertures form. Later formed fractures will tend to abut against the earlier fractures rather than cross-cut, hence Y-node development is favoured over X-node. The power-law fracture distributions are typical of massive crystalline rocks (e.g. Genter *et al.* 1997; Gillespie *et al.* 1999, Odling *et al.* 1999). The long history of brittle deformation and reactivation of structures within the Lewisian gneisses produced areas in which there are multiple fracture sets with power-law size distributions and good connectivity but, as been noted previously, these attributes alone are not enough to make a viable fractured reservoir (Nelson 1985).

Our characterisation demonstrates that certainly the onshore basement terranes provide a good first-order analogue for the offshore Clair basement and greater Rona Ridge. Importantly however, our analysis has also shown that important differences do exist between the areas, e.g. the Hebrides has different aperture scaling to the Mainland and Clair which we discuss in the following sections as it potentially provides further insight into what produces better reservoir potential in the basement gneisses. If it is accepted that our MLE analysis indicates a general power law behaviour for the fracture aperture distributions, the large number of datasets collated in this study enables the overall scaling properties of the distributions to emerge. In most fracture studies there is generally high variability in scaling and fracture intensity between individual sample lines (e.g. see McCaffrey *et al.* 2003). In previous work, we have shown for basement lithologies, at the outcrop scale, that fracture distributions are affected by lithology and proximity to higher order structures. Beacom *et al.* (2001) showed that fracture densities and clustering are higher in metasedimentary rocks compared to the more common intermediate to acidic gneisses. Pless *et al.* (2015) analysed a well exposed basement outcrop in the Rhiconnich terrane and found that fracture density is higher within a 220m envelope adjacent to the Kinlochbervie fault (Fig 2). The outcrop-scale datasets reported in this study are all deliberately taken from intermediate to felsic gneisses which minimises significant variation caused by lithology. This lithology also dominates in the offshore basement (e.g.

Holdsworth *et al.* 2018). The variation in fracture intensity of about an order of magnitude in the outcrop data for the mainland (Assynt and Rhiconich terranes) does include variation due to proximity to major structures (Fig. 3, 4).

An increase in fracture intensity with proximity to major structures explains the difference we see in the variability between the onshore and the offshore datasets. We find that the Clair core aperture dataset, of equivalent scale to the outcrop data, show similar power law scaling to mainland Scotland with exponents in the range of 1-1.2. However, all of the Clair datasets plot in the higher fracture intensity range and do not show the lower intensity patterns displayed by the Mainland. Specifically, the Clair data generally occupy the area defined by the grey box defined in Figure 4 whereas only the higher fracture intensity samples from the Mainland do this – including those closer to major structures like the Kinlochbervie fault (Figs 2 and 4). The Clair fracture intensity data have a much more limited spatial coverage compared to the Mainland fracture sample lines in that they come from a single horizontal well that was drilled close to the top-basement interface; the Clair Ridge fault. Holdsworth *et al.* (2019a) also reported that the Clair core aperture distributions (the same datasets as plotted herein) show a systematic variation with highest fracture intensity in cores taken closest to the top basement interface. The above discussion and the findings of Holdsworth *et al.* (2019a) show that variations in fracture intensity of about an order of magnitude in aperture distributions might be expected due to proximity to major structures. What this variation does not account for is the significant variation in *scaling* (slope of the lines) between the Hebrides aperture datasets and those of the Mainland terranes and Clair. As we have shown in this study, the fracture apertures collected from the Hebrides, from both high and low intensity regions, show significantly lower scaling exponents (in range 0.5-0.8) compared with Clair or the Mainland (1-1.2 (Fig. 4). In simple terms, this means that in any sample we take from the Hebrides, we see more fractures with large aperture and relatively fewer with smaller apertures. Given that the fracture length distributions appear similar for all the datasets, we seek an explanation that can account for the presence of relatively more larger aperture structures in the Hebrides. One

explanation could be that the Hebrides has experienced more Mesozoic faulting, but there is no evidence from the data that the overall fracture intensities are higher here than on the Mainland or at Clair. Using geological observations, we propose a simple conceptual model based on the development of fissures in basement blocks in the near-surface during the Mesozoic in order to account for the scaling differences we observe.

In recent related work, Holdsworth *et al.* (2019a; 2019b) report structures and textures from offshore fracture fills that reveal the widespread development of steeply inclined to sub-vertical, rift-related tensile fissures in the basement lithologies of the Rona Ridge. They suggest that near-surface fissuring during rift-related faulting, as seen in modern rift systems - such as those exposed in Iceland (Kettermann *et al.* 2019) - allowed pervasive influx of clastic sediment fills from above and hydrothermal mineral fills from below. These partial sediment and vuggy mineral fills could act as natural props holding open fracture systems enabling long-term permeability pathways and facilitating hydrocarbon migration (Holdsworth *et al.* 2019a, b). In the following section, we explore whether this model might explain the different scaling properties that we see in onshore-offshore NW Scotland.

Our model is based on the following assumptions: 1) The fracture systems in the Lewisian basement and equivalents offshore are a both cumulative products of multiple episodes of brittle deformation that produced shear, hybrid and tensile fractures; some of which display evidence for reactivation. 2) The basement was exposed at surface during its history for significant periods of time as indicated by the preservation of the basal Torridonian (ca 1.2 Ga Stoer, ca 1.04 Ga Torridan groups), Cambrian (ca 0.5 Ga) and Mesozoic (< 0.3 Ga) unconformities. 3) The basement experienced at least one (most likely several) phases of rifting whilst at surface that produced significant fissure-type fracturing with sediment and mineral infills (e.g. Beacom *et al.* 1999; Jonk *et al.* 2004; Holdsworth *et al.* 2019a, b). The model presented in Figure 8 shows a basement block with cover sediments (representing older sequences such as the Devonian-Carboniferous Clair Group, for

example) that has been deformed by brittle deformation related to rifting. We know that many of the larger fractures onshore in the Hebrides (Franklin 2013) and offshore (Holdsworth *et al.* 2019a, b) are sediment filled, contain vuggy cavities in mineral fills, and show clear evidence for past fluid flow (mineralisation) and even present-day fluid transport. These types of structures have been recorded in other settings where high strength crystalline (e.g. Montenat *et al.* 1991) or carbonate rocks (e.g. Wright *et al.* 2009) are exposed at surface; sub-unconformity fissure fills and related structures are also widely recorded in active rift settings (e.g. Frenzel & Woodcock 2014; Ketterman *et al.* 2016; 2019; Koehn *et al.* 2019).

Analogue modelling studies (e.g. van Gent *et al.* 2010; Holland *et al.* 2011) demonstrate that fissure structures which form open tensile fractures (with sediment infills) at surface, likely change character with depth transitioning through hybrid (shear tensile structures) to shear fractures at depth with a concomitant reduction in consistent fracture aperture. This variation in fissure/fault character with depth becomes important when considering the erosional level of the basement terranes of Scotland and the Rona Ridge at various times in their geological history (Fig. 8). We hypothesise that near surface, large aperture tensile fractures with a more distributed deformation (a lower aperture exponent < 1 and $C_v < 1$) indicate a position near the top of a basement block. For example, a sample from well A-A' in Figure 8, or an onshore exposure located at an equivalent position. In contrast, where the faults and fractures intersected have more of a shear component with damage zones clustered around the larger fault structures (thus aperture exponents > 1 and $C_v > 1$), it indicates that erosion levels are somewhat greater (Well B'-B' in Figure 8 or equivalent exposure). We suggest that less eroded fault blocks represent the Hebridean basement terranes (and perhaps also the basement of Lancaster – see Holdsworth *et al.* 2019b) whereas the Clair basement and the mainland exposure represent more deeply eroded equivalents.

Further work is needed both on subsurface datasets and the onshore analogues to better constrain the speculative model proposed here. This study largely compiles datasets collected prior

to our new understanding of the key role of fissuring in creating viable basement reservoirs. There is a need for new datasets that focus on the fissure structures to test this hypothesis, but at the moment it serves as a semi-quantitative predictor of the fracture attributes and hence also their fluid storage capacities and flow performance. Our model for the Rona ridge, Mainland, and Clair basement fracture systems suggests a possible depth-dependent influence component on the basement fracture systems. Whilst this is primarily due to a downward change in fissure and fault characteristics, it is the appreciation of the depth of erosion of the uplifted fault blocks in each of the rift episodes that is key to understanding the preserved fracture attributes and their influence on reservoir behaviour. Other factors that need to be explored include the effect on fracture attributes of the presence and thickness of cover sequence present during rifting, but our model provides a hypothesis that can be further tested. Fracture characterisation of reservoir analogues can help to reduce uncertainties in the development of subsurface models that are created to determine drilling locations and quantifying the likely economic returns in terms of hydrocarbon production and resource in fractured basement fields such as Lancaster and Clair. However, we agree with Nelson (1985) when he said that 'Finding fractures is not enough'. It is finding where the right *type* of fractures are preserved, in this case places where Mesozoic sub-unconformity fissures have formed, that is key to a good reservoir in the offshore crystalline basement of NW Scotland.

Conclusions

One of the most extensive investigations of fault and fracture attributes collected from brittle structures in the onshore and offshore Lewisian Gneiss Complex rocks of NW Scotland shows that fracture sizes display power-law scaling of aperture and length attributes and are highly connected across a wide range of scales. The results show that the onshore fracture systems may be used as a good analogue for the basement reservoirs of the Rona Ridge and likely other fractured basement reservoirs worldwide. The high connectivity and size attribute scaling characteristics of the faults and fractures that may form in uplifted, crystalline basement rift blocks confirms that given the right

geological history – notably the development and preservation of near surface, rift-related fissure systems beneath unconformities - they may make good reservoir targets in their own right.

Acknowledgements

We thank the Clair Joint Venture, Hurricane Exploration, BP Conoco Phillips, and NERC for supporting this work on basement fracture systems. Casey Nixon is thanked for help with the topological analysis and Geospatial Research Ltd for an early version of Figure 1. We thank reviewer Dave Sanderson, Editor Simon Price and an anonymous reviewer for their insightful comments.

ACCEPTED MANUSCRIPT

References

- Achtziger-Zupančič, P., Loew, S., and Mariéthoz, G. 2017. A new global database to improve predictions of permeability distribution in crystalline rocks at site scale, *J. Geophys. Res. Solid Earth*, 122, 3513– 3539, doi:10.1002/2017JB014106.
- Baecher, G.B., 1983. Statistical analysis of rock mass fracturing. *Journal of the International Association for Mathematical Geology*, 15(2), pp.329-348.
- Beacom, L. E. 1999. The kinematic evolution of reactivated and non-activated Faults in Basement Rocks, NW Scotland. PhD thesis, Queen's University.
- Bai, T., Pollard, D. D., and Gao, H., 2000. Explanation for fracture spacing in layered materials: *Nature*, 403, 753–756.
- Beacom, L., Holdsworth, R. E., McCaffrey, K. J. W. & Anderson, T. 2001. A quantitative study of the influence of pre-existing compositional and fabric heterogeneities upon fracture zone development during basement reactivation. In: Holdsworth, R. E., Strachan, R. A., Magloughlin, J. F. & Knipe, R. J. (eds.) *The nature and tectonic significance of fault zone weakening*. Geological Society Special Publication. 186, 195-211. doi:10.1144/GSL.SP.2001.186.01.12.
- Bonnet, E., O. Bour, N. E. Odling, P. Davy, I. Main, P. Cowie and B. Berkowitz, 2001, Scaling of fracture systems in geological media. *Reviews of Geophysics*, 39, 347–383.
- Bridgwater, D., Watson, J.V. and Windley, B.F., 1973. A Discussion on the evolution of the Precambrian crust-The Archaean craton of the North Atlantic region. *Philosophical Transactions of the Royal Society of London. Series A, Mathematical and Physical Sciences*, 273, 493-512.
- Butler, C.A., Holdsworth, R.E. and Strachan, R.A., 1995. Evidence for Caledonian sinistral strike-slip motion and associated fault zone weakening, Outer Hebrides Fault Zone, NW Scotland. *Journal of the Geological Society*, 152, 743-746.
- Clauset, A., C. R. Shalizi and M. E. Newman, 2009, Power-law distributions in empirical data. *SIAM review*, v. 51, 4, 661-703.
- Coney, D., Fyfe, T. B., Retail, P. & Smith, P. J. 1993. Clair appraisal: the benefits of a co-operative approach, Geological Society, London. *Petroleum Geology of Northwest Europe*. Proceedings of the 4th Conference. J. R. Parker, J.R. (ed). pp. 1409-1420.
- Dichiarante, A.M., McCaffrey, K.J.W., Holdsworth, R.E., Bjørnara T.I. & Dempsey, E.D. 2020. Fault and fracture scaling and connectivity in the Devonian Orcadian Basin and implications for the offshore Clair Field, Scotland. <https://doi.org/10.5194/se-2020-15>
- Ellis, M.A., Laubach, S.E., Eichhubl, P., Olson, J.E. & Hargrove, P., 2012. Fracture development and diagenesis of Torridon Group Applecross Formation, near An Teallach, NW Scotland: millennia of brittle deformation resilience? *J. Geol. Soc. Lond.* 169, 297-310.

Franklin, B.S.G. (2013) Characterising fracture systems within upfaulted basement highs in the Hebridean Islands: an onshore analogue for the Clair Field. Doctoral thesis, Durham University. <http://etheses.dur.ac.uk/7765/> [Accessed 13/05/2020]

Friend, C. R. L. & Kinny, P. D. 2001. A reappraisal of the Lewisian Gneiss Complex: geochronological evidence for its tectonic assembly from disparate terranes in the Proterozoic. *Contributions to Mineralogy and Petrology*, 142, 198–218.

Frenzel, M., and Woodcock, N.H., 2014, Cockade breccia: product of mineralisation along dilational faults: *Journal of Structural Geology*, v. 68, p. 194-206. <https://doi.org/10.1016/j.jsg.2014.09.001>

Genter, A., Castaing, C., Dezayes, C., Tenzer, H., Traineau, H. and Villemin, T., 1997. Comparative analysis of direct (core) and indirect (borehole imaging tools) collection of fracture data in the Hot Dry Rock Soultz reservoir (France). *Journal of Geophysical Research: Solid Earth*, 102, 15419–15431.

Gillespie, P. A., C. B. Howard, J. J. Walsh and J. Watterson, 1993, Measurement and characterisation of spatial distributions of fractures. *Tectonophysics*, 226, 113 – 141.

Gillespie, P.A., Johnston, J.D., Loriga, M.A., McCaffrey, K.J.W., Walsh, J.J. and Watterson, J., 1999. Influence of layering on vein systematics in line samples. Geological Society, London, Special Publications, 155, 35-56.

Gutmanis, J. C. 2009. Basement reservoirs-a review of their geological and production characteristics. In: International Petroleum Technology Conference, IPTC 13156, 7–9 December 2009, Doha, Qatar.

Gutmanis, J. C., Batchelor, T., Doe, S., Pascual-Cebrian E. 2015. Hydrocarbon production from fractured basement formations. GeoSciences Ltd Technical paper https://docs.wixstatic.com/ugd/309073_46b5fc2585a84fdf91bfb679047f7470.pdf [Accessed 24/07/19]

Hardman, K., 2019. Cracking Canisp: Deep void evolution during ancient earthquakes. *Geoscientist* 29, 10-15, <https://doi.org/10.1144/geosci2019-003>; [Accessed 24/07/19]

Healy, D., Rizzo, R.E., Cornwell, D.G., Farrell, N.J., Watkins, H., Timms, N.E., Gomez-Rivas, E. and Smith, M., 2017. FracPaQ: A MATLAB™ toolbox for the quantification of fracture patterns. *Journal of Structural Geology*, 95, 1-16.

Holdsworth, R.E., Morton, A., Frei, D., Gerdes, A., Strachan, R.A., Dempsey, E., Warren, C., and Whitham, A., 2018, The nature and significance of the Faroe-Shetland terrane: Linking Archaean basement blocks across the North Atlantic: *Precambrian Research*, v. 321, p. 154–171, <https://doi.org/10.1016/j.precamres.2018.12.004>

Holdsworth, R.E., McCaffrey, K.J.W., Dempsey, E., Roberts, N.M.W., Hardman, K., Morton, A., Feely, M., Hunt, J., Conway, A., Robertson, A. 2019a. Natural fracture propping and earthquake-induced oil migration in fractured basement reservoirs. *Geology*; 47, 700–704. doi: <https://doi.org/10.1130/G46280.1>

Holdsworth, R.E. Trice, R., Hardman, K., McCaffrey, K.J.W., Morton, A., Frei, D., Dempsey, E, Bird, A, Rogers, S. 2019b. The nature and age of basement host rocks and fracture fills in the Lancaster field

reservoir, West of Shetland. *Journal of the Geological Society, London*,
<https://doi.org/10.1144/jgs2019-142>

Holdsworth, R.E., Selby, D., Dempsey, E., Scott, L., Hardman, K., Fallick, A.E. & Bullock, R. 2020. The nature and age of Mesoproterozoic strike-slip faulting based on Re–Os geochronology of syntectonic copper mineralization, Assynt Terrane, NW Scotland. *Journal of the Geological Society, London*,
<https://doi.org/10.1144/jgs2020-011>.

Holford, S.P., Green, P.F., Hillis, R.R., Underhill, J.R., Stoker, M.S. and Duddy, I.R., 2010. Multiple post-Caledonian exhumation episodes across NW Scotland revealed by apatite fission-track analysis. *Journal of the Geological Society*, 167, 675–694.

Holland, M., Van Gent, H.W., Bazalgette, L., Yassir, N., Hoogerduijn-Strating, E.H., Urai, J.L., 2011. Evolution of dilatant fracture networks in normal faults – evidence from 4D model experiments. *Earth Planetary Science Letters* 304, 399–406. doi: 10.1016/j.epsl.2011.02.017.

Imber, J., Holdsworth, R.E., Butler, C.A. and Strachan, R.A., 2001. A reappraisal of the Sibson-Scholz fault zone model: The nature of the frictional to viscous (“brittle-ductile”) transition along a long-lived, crustal-scale fault, Outer Hebrides, Scotland. *Tectonics*, 20, 601–624.

Imber, J., Strachan, R.A., Holdsworth, R.E. and Butler, C.A., 2002. The initiation and early tectonic significance of the Outer Hebrides Fault Zone, Scotland. *Geological Magazine*, 139, 609–619.

Jonk, R., Kelly, J. and Parnell, J. 2004. The origin and tectonic significance of Lewisian- and Torridonian-hosted clastic dykes near Gairloch, NW Scotland. *Scottish Journal of Geology*, 40, 123–130.

Kettermann, M., von Hagke, C., van Gent, H.W., Gruetzner, C., Urai, J.L., 2016. Dilatant normal faulting in jointed cohesive rocks: a physical model study. *Solid Earth* 7, 843–856.

Kettermann, M., Weismüller, C., von Hagke, C., Reicherter, K., Urai, J.L. 2019 Large near-surface block rotations at normal faults of the Iceland rift: Evolution of tectonic caves and dilatancy. *Geology*, 47 781–785. doi: <https://doi.org/10.1130/G46158.1>

Kinny, P. D., Friend, C. R. L. & Love, G. J. 2005. Proposal for a terrane-based nomenclature for the Lewisian Gneiss Complex of NW Scotland. *Journal of the Geological Society*, 162, 175–186.

Kinny, P.D., Strachan, R.A., Fowler, M., Clark, C., Davis, S., Jahn I., Taylor, R.J.M., Holdsworth, R.E. and Dempsey, E. 2019. The Neoproterozoic Uyea Gneiss Complex, Shetland: an onshore fragment of the Rae Craton on the European Plate. *Journal of the Geological Society, London*, 176, 847–862,
<https://doi.org/10.1144/jgs2019-017>

Koehn, D., Steiner, A. and Aanyu, K., 2019. Modelling of extension and dyking-induced collapse faults and fissures in rifts. *Journal of Structural Geology*, 118, 21–31.

Krabbendam, M. & Leslie, A. (2010) ‘Lateral variations and linkages in thrust geometry: the Traligill transverse zone, Assynt Culmination, Moine thrust belt, NW Scotland’, In: Law, R. D., Butler, R. W. H., Holdsworth, R. E., Krabbendam, M. & Strachan, R. A. (eds) *Continental Tectonics and Mountain Building: The Legacy of Peach and Horne*. Geological Society, London, Special Publications, 335, 335–357. <https://doi.org/10.1144/sp335.16>

- Laubach, S.E. and Diaz-Tushman, K., 2009. Laurentian palaeostress trajectories and ephemeral fracture permeability, Cambrian Eriboll Formation sandstones west of the Moine Thrust Zone, NW Scotland. *Journal of the Geological Society*, 166, 349-362
- Laubach, S. E., 2003, Practical approaches to identifying sealed and open fractures, *AAPG Bulletin*, 87, 561-579.
- Laubach, S.E. and Marshak, S., 1987. Fault patterns generated during extensional deformation of crystalline basement, NW Scotland. *Geological Society, London, Special Publications*, 28, 495-499.
- Massiot, C., McNamara, D.D. and Lewis, B., 2015. Processing and analysis of high temperature geothermal acoustic borehole image logs in the Taupo Volcanic Zone, New Zealand. *Geothermics*, 53, 190-201.
- Mauldon, 1994, Intersection probabilities of impersistent joints. In *International journal of rock mechanics and mining sciences & geomechanics abstracts*, 31, 107-115.
- McCaffrey, K. J. W., & Johnston, J. D. 1996. Fractal analysis of a mineralised vein deposit: Curraghinalt gold deposit, County Tyrone. *Mineralium Deposita*, 31, 52-58.
- McCaffrey, K.J.W., Sleight, J.M., Pugliese, S. and Holdsworth, R.E., 2003. Fracture formation and evolution in crystalline rocks: Insights from attribute analysis. *Geological Society, London, Special Publications*, 214, 109-124.
- Mason, A.J. and Brewer, T.S., 2004. Mafic dyke remnants in the Lewisian Complex of the Outer Hebrides, NW Scotland: a geochemical record of continental break-up and re-assembly. *Precambrian Research*, 133, 121-141.
- Marrett, R., Gale, J.F., Gómez, L.A. and Laubach, S.E., 2018. Correlation analysis of fracture arrangement in space. *Journal of Structural Geology*, 108, 16-33.
- Montenat, C., Barrier, P. and d'Estevou, P.O., 1991. Some aspects of the recent tectonics in the Strait of Messina, Italy. *Tectonophysics*, 19, 203-215.
- Narr, W., 1991, Fracture Density in the Deep Subsurface: Techniques with Application to Point Arguello Oil Field (1). *AAPG bulletin*, 75, 8, 1300-1323.
- Nelson, R.A., 1985, *Geologic Analysis of Naturally Fractured Reservoirs (Contributions in Petroleum Geology and Engineering; v.1)*. Gulf Publishing Company, Houston, 320 p.
- Odling, N.E. 1992. Network properties of a two-dimensional natural fracture pattern. *Pure and Applied Geophysics*, 138, 95-113.
- Odling, N.E., Gillespie, P., Bourguine, B., Castaing, C., Chiles, J.P., Christensen, N.P., Fillion, E., Genter, A., Olsen, C., Thrane, L. and Trice, R., 1999. Variations in fracture system geometry and their implications for fluid flow in fractures hydrocarbon reservoirs. *Petroleum Geoscience*, 5, 373-384.
- Olson, J. E., 2007, Fracture aperture, length and pattern geometry development under biaxial loading: a numerical study with applications to natural, cross-jointed systems. *Geological Society, London, Special Publications*, 289, 123-142.

- Ortega, O.J., Marrett, R.A. and Laubach, S.E., 2006. A scale-independent approach to fracture intensity and average spacing measurement. *AAPG Bulletin*, 90, 193-208
- Park, R. G. 1970. Observations on Lewisian Chronology. *Scottish Journal of Geology*, 6, 379-399.
- Park, R.G., Stewart, A.D., Wright, D.T. and Trewin, N.H., 2002. The Hebridean terrane. *The Geology of Scotland. Geological Society, London*, 45, p.80.
- Pless, J. C. 2012. Characterising fractured basement using the Lewisian Gneiss Complex, NW Scotland: implications for fracture systems in the Clair Field basement. PhD thesis, Durham University, <http://etheses.dur.ac.uk/3489/> [Accessed 13/05/2020]
- Pless, J.C., McCaffrey, K.J.W., Jones, R.R., Holdsworth, R.E., Conway, A. and Krabbendam, M., 2015. 3D characterization of fracture systems using terrestrial laser scanning: An example from the Lewisian basement of NW Scotland. *Geological Society, London, Special Publications*, 421, 125-141.
- Priest, S.D. and Hudson, J.A., 1981. Estimation of discontinuity spacing and trace length using scanline surveys. In *International Journal of Rock Mechanics and Mining Sciences & Geomechanics Abstracts* 18, 183-197)
- Ritchie, J.D., Noble, D., Darbyshire, F., Millar, I., Chambers, L., 2011. Pre-Devonian. BGS Research Report RR/11/01 In: Ritchie, J.D., Ziska, H., Johnson, H., Evans, D. (Eds.) *Geology of the Faroe-Shetland Basin and Adjacent Areas*, pp. 71–78.
- Rizzo, R.E., Healy, D. and De Siena, L., 2017. Benefits of maximum likelihood estimators for fracture attribute analysis: Implications for permeability and up-scaling. *Journal of Structural Geology*, 95, 17-31.
- Roberts, A.M. and Holdsworth, R.E., 1999. Linking onshore and offshore structures: Mesozoic extension in the Scottish Highlands. *Journal of the Geological Society*, 156, 1061-1064.
- Rohrbaugh Jr, M.B., Dunne, W.M. and Mauldon, M., 2002. Estimating fracture trace intensity, density, and mean length using circular scan lines and windows. *AAPG bulletin*, 86, 2089-2104.
- Sanderson, D.J. and Nixon, C.W., 2015. The use of topology in fracture network characterization. *Journal of Structural Geology*, 72, 55-66.
- Sibson, R. H. 1977. Fault rocks and fault mechanisms. *Journal of the Geological Society*, 133, 191-213.
- Slightam, C. 2012. Characterizing seismic-scale faults pre- and post-drilling; Lewisian Basement, West of Shetlands, UK. In: Spence, G. H., Redfern, J., Aguilera, R., Bevan, T. G., Cosgrove, J. W., Couples, G. D. & Daniel, J. M. (eds) *Advances in the Study of Fractured Reservoirs. Geological Society, Special Publications*, 374. <http://dx.doi.org/10.1144/SP374.6>
- Steel, R.J. & Wilson, A.C., 1975. Sedimentation and tectonism (? Permo-Triassic) on the margin of the North Minch Basin, Lewis. *Journal of the Geological Society*, 131, 183-200.
- Stoker, M.S., Holford, S.P. and Hillis, R.R., 2018. A rift-to-drift record of vertical crustal motions in the Faroe–Shetland Basin, NW European margin: establishing constraints on NE Atlantic evolution. *Journal of the Geological Society*, 175, 263-274.

Sutton, J. & Watson, J. 1951. The pre-Torridonian metamorphic history of the Loch Torridon and Scourie areas in the North-West Highlands, and its bearing on the chronological classification of the Lewisian. *Quarterly Journal of the Geological Society*, 106, 241-307.

Trice, R. 2014. Basement exploration West of Shetlands, progress in opening a new play on the UKCS. In: Cannon, S.J.C. & Ellis, D. (eds) *Hydrocarbon Exploration to Exploitation West of Shetlands*. Geological Society, London, Special Publications, 397, 81–105, <https://doi.org/10.1144/SP397.3>

Trice R., Hiorth., C Holdsworth R.E. 2019. Fractured basement play development in the UK and Norwegian rifted margins: a discussion and implications for exploitation. In: Jackson, C. A-L. (editor) *Cross-Border Petroleum Geology and Exploration: The British and Norwegian Continental Margins*. Geological Society of London, Special Publication, 495.

van Gent, H.W., Holland, M., Urai, J.L., and Loosveld, R., 2010, Evolution of fault zones in carbonates with mechanical stratigraphy - insights from scale models using layered cohesive powder. *Journal of Structural Geology*, v. 32, p. 1375-1391, doi: 10.1016/j.jsg.2009.05.006.

Walsh, J. J. and J. Watterson, 1993, Fractal analysis of fracture patterns using the standard box-counting technique: valid and invalid methodologies. *Journal of Structural Geology*, 15, 1509–1512.

Wang, Q., Laubach, S.E., Gale, J.F.W. and Ramos, M.J., 2019. Quantified fracture (joint) clustering in Archean basement, Wyoming: application of the normalized correlation count method. *Petroleum Geoscience*, 25, 415-428.

Watkins, H., Bond, C.E., Healy, D. and Butler, R.W., 2015. Appraisal of fracture sampling methods and a new workflow to characterise heterogeneous fracture networks at outcrop. *Journal of Structural Geology*, 72, 67-82.

Wheeler, J., Park, R.G., Rollinson, H.R. and Beach, A., 2010. The Lewisian Complex: insights into deep crustal evolution. Geological Society, London, Special Publications, 335. 51-79. Whitehouse 1993.

Wright, V., Woodcock, N.H. and Dickson, J.A.D., 2009. Fissure fills along faults: Variscan examples from Gower, South Wales. *Geological Magazine*, 146,890-902.

Zeeb, C., Gomez-Rivas, E., Bons, P.D. and Blum, P., 2013. Evaluation of sampling methods for fracture network characterization using outcrops. *AAPG bulletin*, 97, 1545-1566.

Figure Captions

Figure 1. Map of the NW UK continental shelf showing location of fields, prospects, top basement depth map offshore and onshore crystalline basement exposures.

Figure 2. Lineament interpretation for well exposed parts of the Mainland and Hebrides basement of NW Scotland. Outcrop fracture sample sites are labelled and shown in blue (Hebrides), light green (Mainland – Rhiconnich terrain) and dark green (Assynt terrain). Summary rose diagrams of fracture

orientations for the Mainland and Hebrides. Inset map shows Clair field (outline of Clair first development phase in black line) with lineaments from Pless (2012). Underlying onshore geology from BGS 1:625,000 geology map. Main units include Neoproterozoic with/without Palaeoproterozoic (Laxfordian) overprint: A = intermediate to granitic gneiss (Lewisian), Paleoproterozoic: Z = felsic intrusive rocks, Zm = Mafic intrusive rocks, Zs = metasedimentary rocks, M = Moine metasediments, Mesoproterozoic: S = Stoer Gp, Neoproterozoic: T = Torridonian, CO = Cambro-Ordovician sedimentary rocks, OS = Ordovician/Silurian alkaline syenite, F= fault rocks (mylonites, cataclasites and pseudotachylytes), PT = Permo-Triassic sedimentary rocks. Major structures are labelled – KLB F = Kinlochbervie fault.

Fig. 3. Typical basement fracture types and fills. (a) closely spaced laterally and vertically extensive jointing in granitic gneiss Lewisian basement, Uyea, Shetland (see Kinny *et al.* 2019). Note that later Devonian-age dykes have exploited these well-developed joint systems. (b) Composite carbonate veins cutting mafic gneisses, Traigh Dhail Mor, Isle of Lewis (for location, see Fig. 2). Note large open vug (V). (c) Cross sectional view of part of a ca 30m wide fissure filled with chaotic mm- to m-sized angular clasts of basement, and possible red sediment locally cemented by carbonate. Age of fill uncertain, but note that the contact with the wall rock has been exploited by a Cenozoic basalt dyke, suggesting that the breccia is likely Mesozoic in age. Traigh Dhail Mor, Isle of Lewis. (d) Close-up view of crudely laminated nature of the fill at Traigh Dhail Mhor suggesting an element of water-lain deposition. (e) Fissure filled with chaotic collapse breccia where the matrix is cataclasite and pseudotachylyte, Canisp Shear Zone, Achmelvich. Note that in this case, the development of the dilational cavity is thought to be related to seismogenic slip events along the well-developed foliation in the wall rocks at depths >5 km (see Hardman 2019 for details). (f) Foliated multicoloured gouges and breccias from the core of the Seaforth Fault, a major N-S Mesozoic normal fault with km-scale offsets that cuts the Isle of Lewis (Fig. 2; see Franklin 2013 for details).

Figure 4. Fracture aperture intensity data for: a) Mainland Scotland; b) Hebrides; and c) Clair basement. The grey polygon highlights the same Fracture Intensity/Aperture space with a slope of -1 and is shown for comparison in each plot. Orange bars show comparative fracture intensity ranges for 10mm aperture fractures as discussed in text. Data from locations that sample Mesozoic structures on the Hebrides include Garrabost, Memorial Cairn, Pabail, Seisadar, and Tolstadh.

Figure 5. Two measures of fracture length intensity scaling. a) Fracture lengths intersected in 1D samples plotted on a multi-scale diagram from Mainland outcrops and the Clair top-basement seismic attribute map. b) The intensity of fractures per unit area (m) is shown for 2D length data from window samples taken across Mainland, Hebrides and Clair seismic attribute and topographic maps.

Figure 6. Plot of Coefficient of variation (C_v) versus Fracture Intensity for outcrop, mesoscale (virtual model) and regional (lineament maps) datasets from Mainland (Assynt and Rhiconich), Hebrides and Clair.

Figure 7. Fracture topology results from Clair drill core samples, the greater Rona ridge, and the Assynt Terrane (outcrops and regional lineament samples). Examples of the three scales sampled are shown: regional scale; outcrop scale; and core scale.

Figure 8. Conceptual model for fracture systems and their attributes developed in an uplifted basement block (see also Holdsworth *et al.* 2019b). Cartoon logs A'-A' and B-B' correspond to 2 hypothetical, horizontally deviated wells drilled through the block at different structural levels or through their onshore analogue equivalents exposed in outcrop.

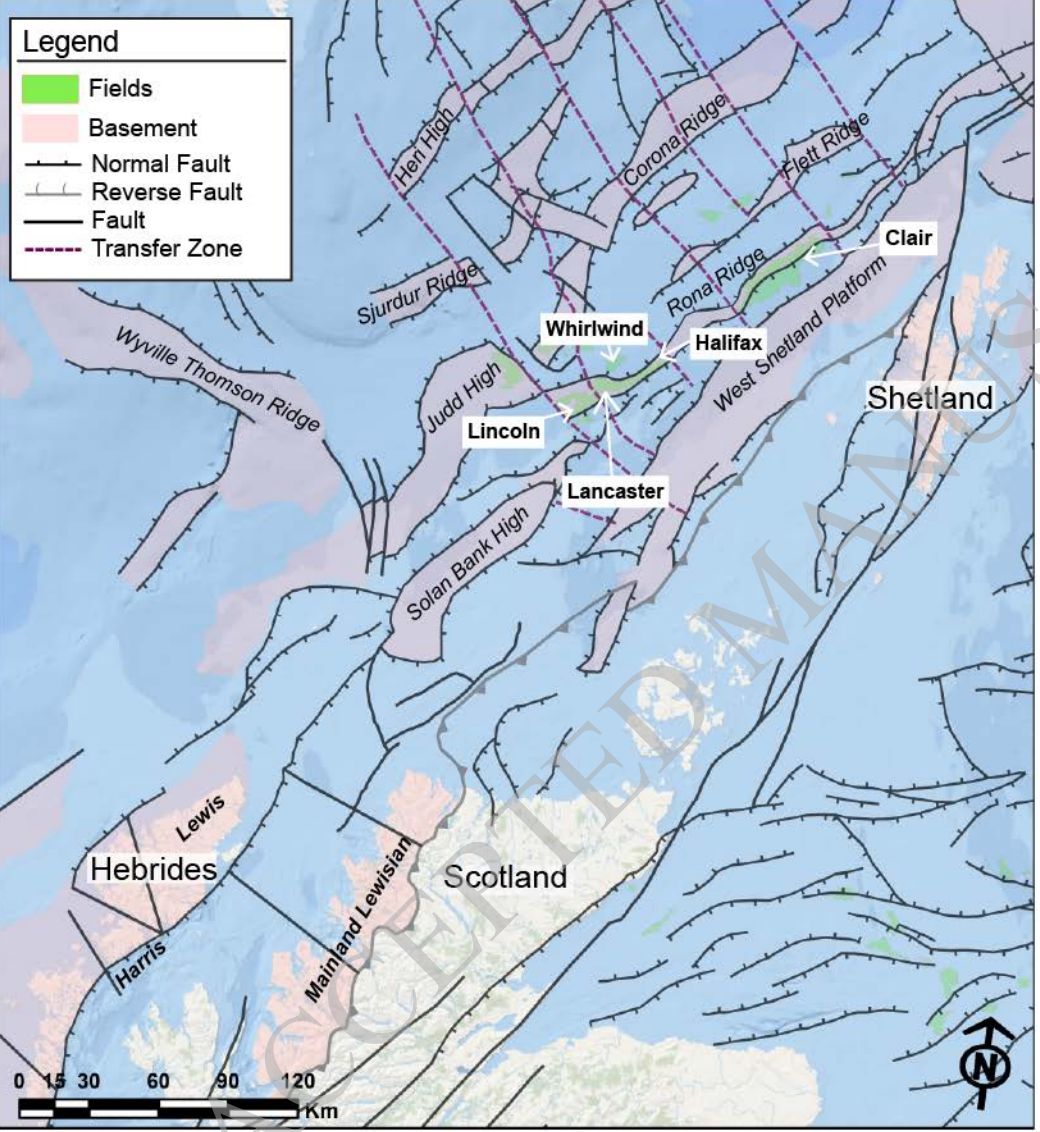
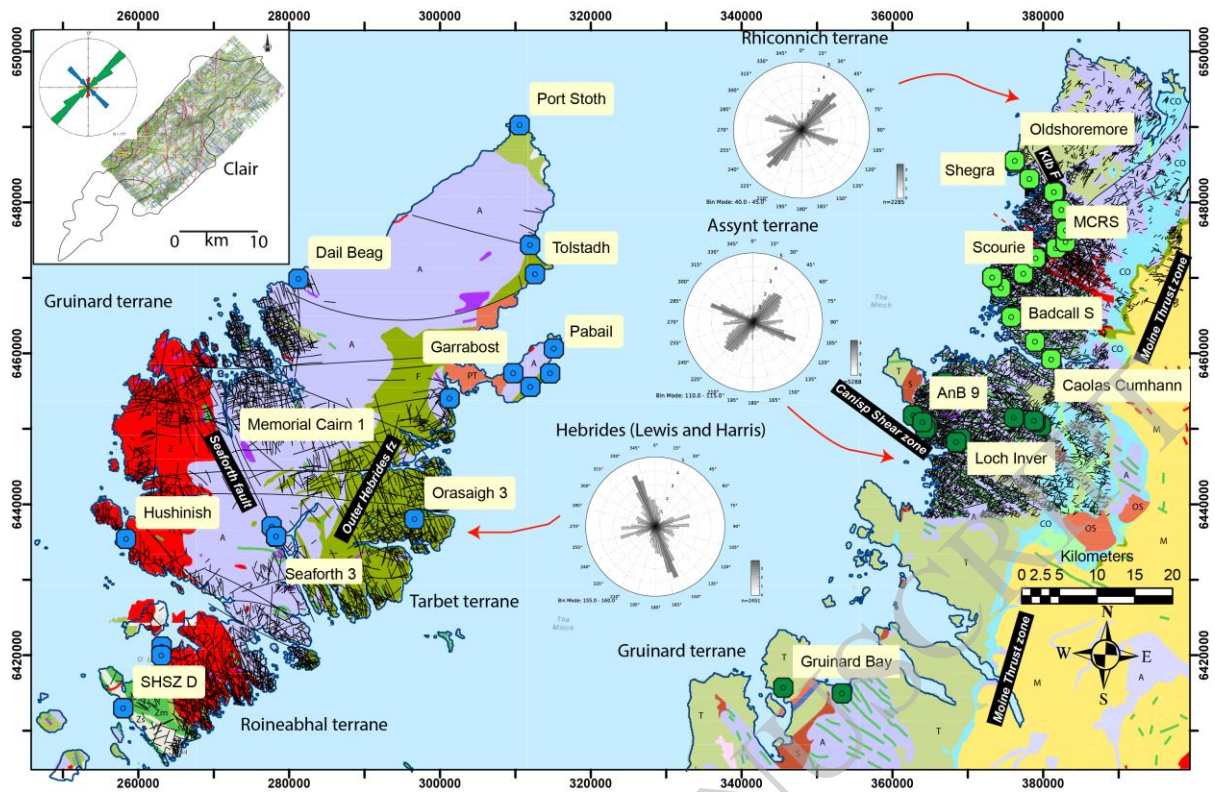
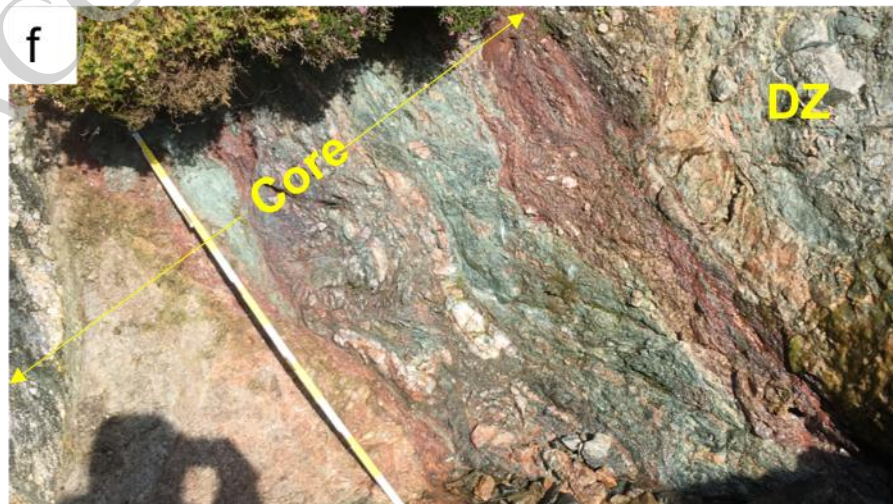
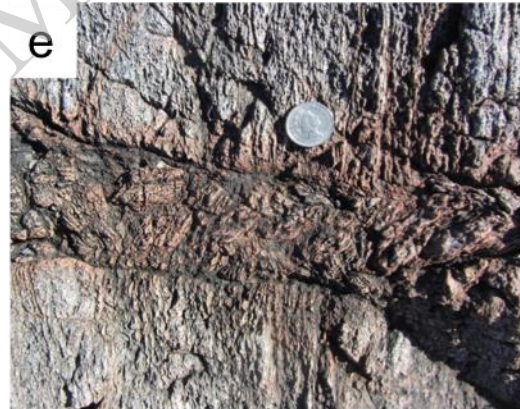
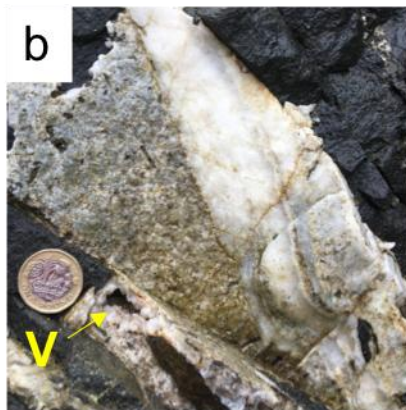


Fig. 1





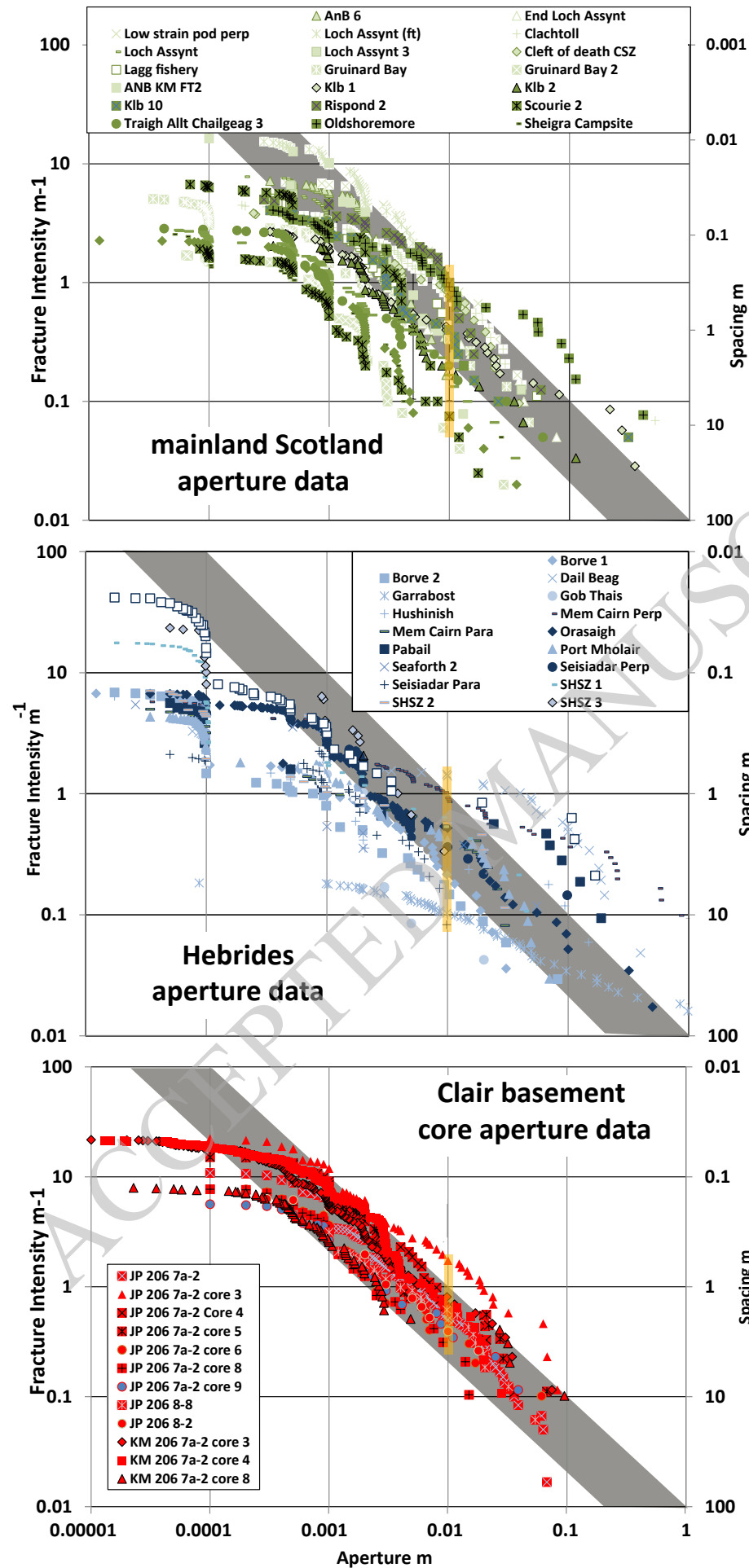
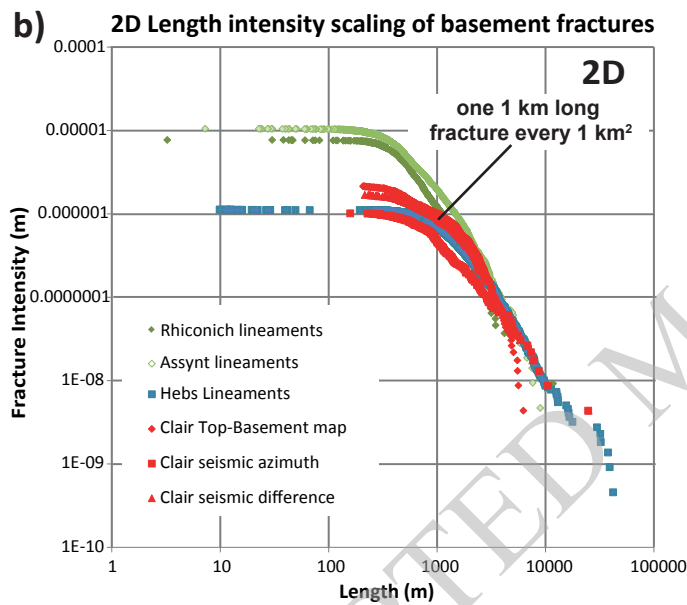
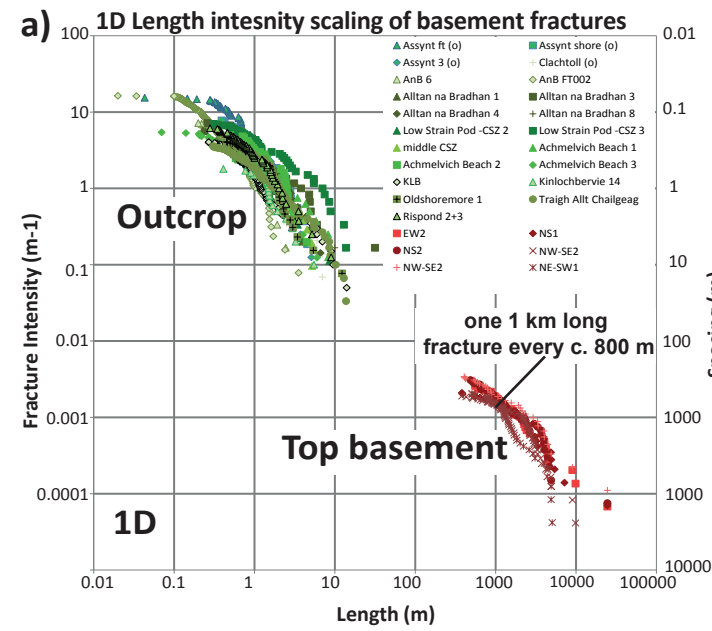


Fig 4



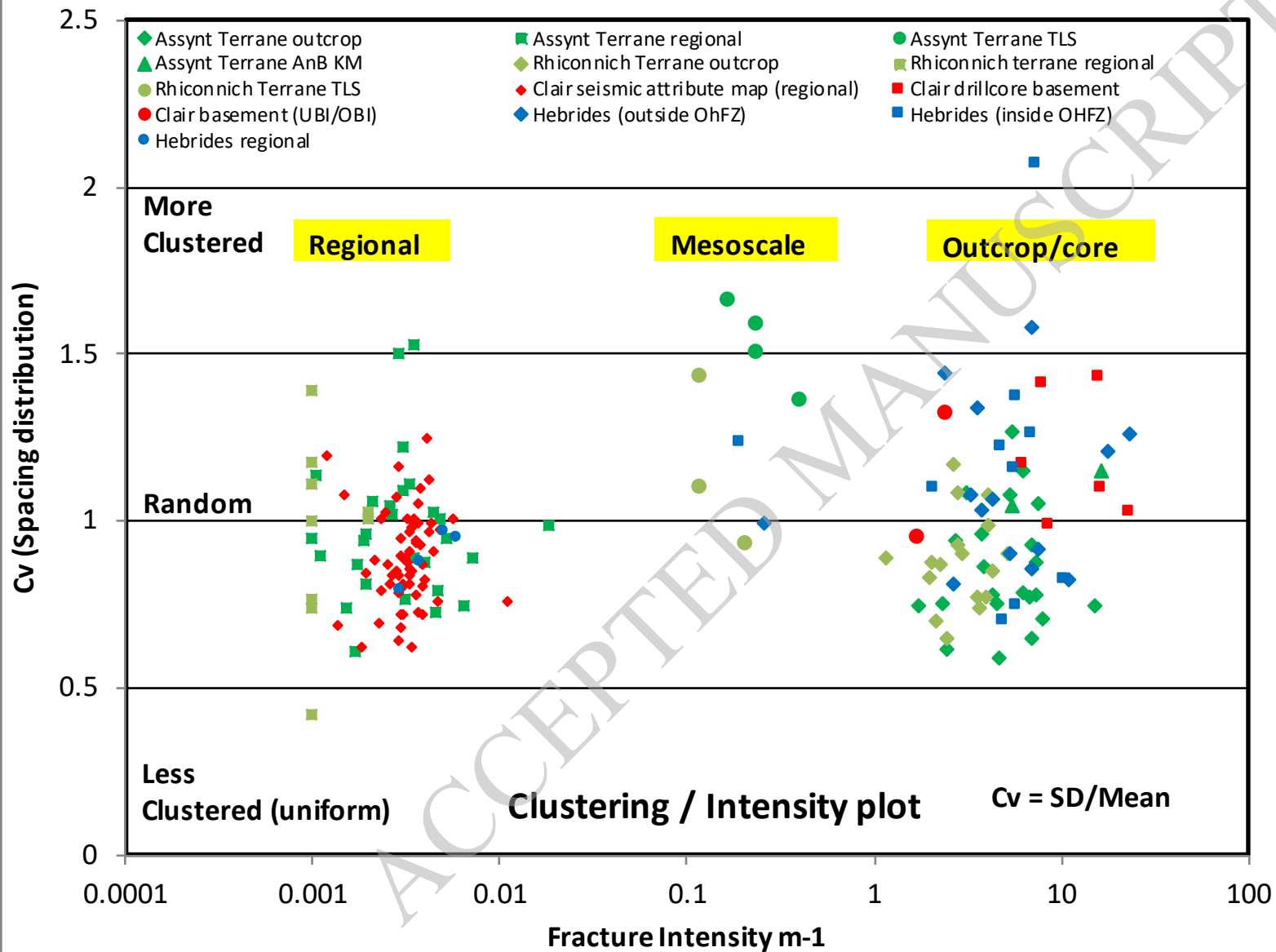
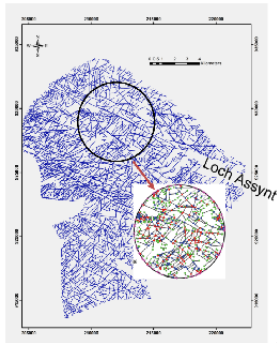


Fig.7

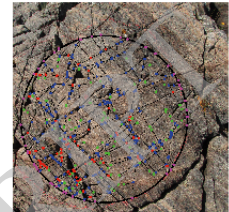
Regional scale

(Assynt Regional) 7.5 km circle



Outcrop scale

ANB T2 (2m circle)



Core scale

(RR4 7.5 cm circle)

